Influence of malformation of right coronary artery originating from the left sinus on the hemodynamic environment

Mengyang Cong
Shandong University of Science and Technology
Xingming Xu
Shandong University of Science and Technology
Jianfeng Qiu
Shandong First Medical University & Shandong Academy of Medical Sciences
Shun Dai
Shandong Jiaotong University
Chuanzhi Chen
Tongji University School of Medicine
Xiuqing Qian
Capital Medical University
Hongbin Zhang
Shandong University of Science and Technology
Shengxue Qin
Shandong University of Science and Technology
Huihui Zhao (HHZhao1029@163.com)
https://orcid.org/0000-0002-3478-7134

Research

Keywords: Computational fluid dynamics, Anomalous right coronary artery, volumetric flow, Pressure, Wall shear stress, Statistical analysis

Posted Date: January 30th, 2020

DOI: https://doi.org/10.21203/rs.2.22271/v1

Version of Record: A version of this preprint was published on July 29th, 2020. See the published version at https://doi.org/10.1186/s12938-020-00804-0.

Abstract

Background: The Anomalous origin of the Right Coronary Artery (RCA) from the Left Coronary artery sinus(AORL) is one of the abnormal origins of the coronary arteries. Most of these issues seldom have effects on human health, but some individuals may have symptoms such as myocardial ischaemia or even sudden death. Recently, researchers are studying AORL through clinical cases, but study based on computational fluid dynamics (CFD) is rarely seen. In this study, haemodynamic changes between normal origin of the RCA and AORL are compared according to numerical simulation results.

Methods: Realistic three-dimensional models of 16 normal right coronary arteries and 26 abnormal origins of the right coronary arteries were reconstructed, respectively. The blood flow was numerically simulated using software ANSYS. This study involves one-way fluid-solid coupling finite element model in which the blood is assumed to be incompressible Newtonian fluid, and the vessel is assumed to be isotropic, linear elastic material.

Results: The differences of the cross-sectional area at the inlet between the normal group and the abnormal group was significant ($P < 0.0001$). There were significant differences in the volumetric flow ($P < 0.0001$) and the pressure ($P = 0.0001$). There were positive correlations with the ratio of the cross-sectional area of the RCA to the inlet area of the ascending aorta (AAO) and the ratio of the inlet volumetric flow of the RCA to the volumetric flow of the AAO, in both the normal ($P = 0.0001$, $r = 0.8198$) and abnormal ($P = 0.0199$, $r = 0.4925$) group.

Conclusion: This study shows that the cross-sectional area of the inlet of AORL may cause ischaemia symptoms, and the results may contribute to the further understanding of the clinical symptoms of AORL based on the haemodynamics.

Background

The coronary artery originating from the root of the aorta is divided into the left coronary artery (LCA) and the right coronary artery(RCA). The RCA originating from the right aortic sinus of the heart supplies blood to the superior and inferior ventricles at the right side of the heart. Anomalous origin of the coronary artery (AAOCA) is a common type of congenital coronary artery anomaly[1]. Although some children are born with AAOCA, it may not be diagnosed during coronary angiography until the individual grows to an adolescent or adult [2-4]. There are four main types of AAOCA: (a) absence of the left main artery, (b) abnormal origin of the coronary artery from the improper sinus, (c) anomalous coronary ostium outside of the Valsalva's sinus, and (d) a single coronary artery[5]. Although most coronary artery anomalies have little effects on individuals, some young people who are prone to sudden cardiac death usually have the two common characteristics of abnormal: RCA and abnormal LCA[6]. This study focused on the hemodynamics of the right coronary artery originating from the left coronary sinus.

In patients undergoing coronary angiography the incidence of anomalous origin of the right coronary artery from the left esinus (AORL) is 0.92%[7]. Compared with the origin of LCA, AORL causes a lower rate

of sudden death. The incidence of typical angina and myocardial infarction in patients with a low interarterial course of AORL is significantly lower than that with a high interarterial course in patients [8]. However, even if the incidence of cardiovascular disease due to AORL is relatively low, the consequences are often fatal.

A study reported that AORL can cause myocardial ischaemia, angina pectoris, myocardial infarction, and sudden cardiac death (SCD) [9-11]. The researchers find that an acute angle of AORL may cause cardiovascular disease during exercise [12]; the most proximal part of the artery has an oblique intramural course with a slit-like ostium, which may cause ischaemia [13]. Mechanical compression of the RCA due to the dilation of the pulmonary artery and aorta may result in ischaemia during maximal exercise [14, 15].

Initially, one of the causal mechanism of SCD is considered to be associated with a slit-like or flap-like closure of the orifice[16, 17]. The reported data from the large series of intravascular ultrasonography (IVUS)- based clinical studies in 63 adult patients with AORL have shown evidence that the severity of stenosis relates with the occurrence of ischemic symptoms (ie, syncope, angina, or dyspnea, in addition to SCD) [18]. The cross-sectional area at the inlet of RCA of the abnormal group is much smaller than that of the normal group in this study. One of the features of AORL is a slit-like orifice [19], so The cross-sectional area is small. The factor may cause a functional stenosis of AORL, ischemia and malignant ventricular arrhythmias [20].

In this paper, the haemodynamics of AORL were studied based on computational fluid dynamics (CFD). As a branch of hydrodynamics, CFD is increasingly being applied in biomedical engineering. Many bioengineers have used CFD to study complex cardiovascular diseases, such as coronary artery stenosis [21-26].

In this study, we hypothesised that the the hemodynamics of the right coronary artery of normal origin differed from that of AORL. 42 realistic geometic models of AORL were reconstructed based on computed tomography (CT) scan images, and then the haemodynamic was simulated with numerical method . The main purpose of this study was to investigate the effects of AORL on haemodynamics, and it provided theoretical significance for clinical evaluation of ischemic symptoms.

Results

Before ANSYS analysis, the material parameters are set as follows: the blood density and viscosity were set to be constant at 1060 kg/m^3 and 3.5×10^{-3} Pa•s, respectively[27]. The vessel wall density is 1150 kg/m^3, the Young's modulus is 5 MPa, and the Poisson's ratio is 0.45[28].

The red section is the cross-sectional of the inlet of the RCA (Fig. 3). The flow rate of AORL was smaller than that of the normal coronary artery(Fig. 4). The average pressure and WSS at the corner of the RCA in each model were calculated by five-spot sampling. The gray part is the range of the five-point sampling method and its length is about 10~15mm(Fig. 5).

According to the hemodynamic parameters of the abnormal group, one case of right coronary artery stenosis and three cases of right coronary artery originating from the ascending aorta were removed, and the data of the remaining cases were statistically analyzed. The ratio of the cross-sectional area of the RCA to the inlet area of the ascending aorta (AAO) was defined by:

$S_{\%}=S_{RCA}/S_{AAO.}$

the ratio of the inlet volumetric flow of the RCA to the volumetric flow of the AAO was defined by:

$Q_{\%}=Q_{RCA}/Q_{AAO.}$

In the abnormal group, there were obvious positive correlations with S% and Q% (P=0.0199, r=0.4925) (Fig. 6 (a)). The S% of normal group has a great positive correlation with Q% (P=0.0001, r=0.8198) (Fig. 6 (b)). There were significant differences in the the cross-sectional area of the inet (P<0.0001) (Fig. 7 (a)). The average cross-sectional area of the normal group (12.97±1.253 mm^2) was twice that of the abnormal group (6.314±1.253 mm^2)..The differences of the volumetric flow rates (P<0.0001) and the pressure (P=0.0001) between the normal group and the abnormal group was obvious (Fig. 7 (b), (c)). The average volume flow in the abnormal group (1.119±0.5739 m/s) was about one third of that in the normal group (3.672±0.5739 m/s). The average pressure in the normal group (476.1±77.19 Pa) was about three times that in the abnormal group (146.2±77.19 Pa). No significant difference was observed for WSS (P>0.05) (Fig. 7 (d)). The average WSS of the normal group (2.487±0.7097 Pa) was almost the same as that of the abnormal group (2.590±0.7097 Pa).

Discussion

AORL has been studied by most researchers through clinical cases and anatomical studies, but few studies explored quantitative analyses of haemodynamics to investigate this problem[29-33]. To study the difference in haemodynamics between the normal right coronary artery and AORL, we simulated human coronary artery haemodynamics (the model includes left coronary arteries and RCAs and a partial aorta) based on multi-slice CT scan images. The effects of a slit like closure of AORL on hemodynamic parameters and clinical symptoms were studied by comparing the inlet volumetric flow, pressure and WSS data for the RCA.

The correlation between area ratio and flow ratio was analyzed to eliminate individual vascular differences in each patient. In this study, we proved that Q% decreased with the decrease of S% in both normal and abnormal groups In the abnormal group, although the S% of 4 cases was relatively large, the Q% was relatively small, which may be caused by the small acute angle. In this paper, we also find that the S% and Q% of the abnormal group are smaller than those of the normal group. One reason for this is that although the velocity increased due to a decrease in the cross-sectional area of the inlet of AORL, the volumetric flow into the RCA in abnormal group was three times smaller than that in the normal group, finally; Another reason may be that blood is forced into the LCA, which is caused by the close proximity of the starting position of the LCA and the RCA. In the abnormal group, the volumetric flow into the RCA is

smaller. This leads to insufficient blood flow to the end of the right coronary artery, which is unable to exchange blood with the heart in time. It can eventually lead to myocardial ischaemia, such as angina [34].

Recently research found that the decrease in pressure of coronary artery stenosis compared with that of non-stenosis coronary arteries according to the comparison of hemodynamic parameters between the two groups of coronary artery stenosis and no stenosis[35]. In this work, we proved that the cross-sectional area of the inlet the abnormal group was smaller than that of the normal group, and the pressure at the corner of the abnormal group was smaller than that of the normal group. Fluid energy is composed of potential energy, pressure energy and kinetic energy. A decrease in the cross-sectional area of the abnormal group lead to an increase in the velocity. According to the conservation of energy, the pressure is reduced, which is the same as the results of this study. The second reason for the lower pressure in the abnormal group may also be that the acute take-off angle of AORL results in pressure loss caused by blood flow as it enters the RCA. If the entrance of the RCA is very narrow, it can decrease blood flow to the heart, especially when it is beating hard. Eventually, the decreased blood flow may cause shortness of breath, angina, or other coronary artery disease signs and symptoms [36, 37].

Pathological studies on Coronary artery disease suggest that atherosclerosis is the main cause of myocardial ischaemia in adult population [38]. WSS plays an important role in the development and rupture of atherosclerosis rupture[39]. The study found that the arterial WSS reduction has a positive correlation with the decreasing of artery wall elasticity, and WSS can be one of effective parameters for early diagnosis of atherosclerosis[40, 41]. In this study, we proved that the mean value of WSS between the abnormal group and the normal group was not significantly different. We believe that neither a slit-like or flap-like closure nor the acute take-off angle will affect WSS of the RCA in AORL. Therefore, AORL does not increase the incidence of atherosclerosis.

There are some limitations of this study. Notably, the results indicated that the WSS was more accurate when using the heart arterial cycle as the inlet flow[42]. In future studies, we will perform additional statistical analyses using the cardiac arterial cycle for bidirectional fluid-solid coupling.

Conclusion

The main purpose of this study was to analyse the haemodynamics of AORL using CFD. The results revealed that AORL led to a decrease in the volumetric flow and pressure at the RCA, but there were no differences in the WSS. We concluded that the cross-sectional area of the inlet of AORL, which changed the haemodynamic environment, could cause ischaemia. This study concentrated on the clinical symptoms of the cross-sectional area of the inlet and elucidated that the slit-like orifice may be a reason for ischemic symptoms from a haemodynamic perspective. This study provides useful guidance for clinicians in the diagnosis of AORL.

Materials And Methods

Image collection

16 normal coronary arteries and 26 abnormal coronary arteries CT images were collected based on a 128-slice Siemens (SOMATOM Definition Flash) dual-source CT scanner (80 kV, 140 kV). The tube voltage was selected according to the Body Mass Index (BMI) as follows: if BMI≤18, tube voltage is 80 kV; if 18<BMI≤22, tube voltage is 100 kV; if 22<BMI≤27, tube voltage is 120 kV and if BMI>27, tube voltage is 140 kV. The contrast injection rate is 5-5.5 ml/s, and its dose is 60-80 ml. All patients did not use any drugs to control heart rate before scanning. They took 0.5 ml of nitroglycerin under the tongue before scanning, and they were scanned after breath training in calm state. Scan settings are listed in Table 1.

Artery models

The realistic coronary arterial models were reconstructed based on the collected samples with software Mimics (v9.0, Materialise, Ann Arbor, MI, USA). Geomagic Studio 2013 (3D Systems, Morrisville, NC, USA) was used to smooth the rough surfaces of the reconstructed models and generate solid surfaces subsequently. To make the numerical simulation easier, the small coronary branches of the coronary arterial models were removed. The main branch of right coronary artery was retained, and left anterior descending coronary artery, left main coronary artery and left circumflex coronary artery were retained for the left coronary artery. The ascending aorta was cut off about 0.55 centimeters away from the coronary sinus which is taken as the inlet of blood flow. The surface of reconstructed model was offset 0.5mm along the normal direction to get the outer wall of the vascular. A 3D CAD software, Solidworks (Solidworks Corporation, Boston, MA, USA), was used to rebuild the vessel wall of the model. The vessel wall was created by the reconstruction of the blood solid and the offset solid. The blood model is shown in Fig. 1.

Assumption and governing equations

Blood was considered as a homogenous, incompressible and Newtonian fluid[24]. Blood was assumed to be isothermal. The blood flow was described by the three-dimensional incompressible Navier-Stokes equations and continuity equation [43]:

$$\frac{\partial u}{\partial t} + (u \cdot \nabla)u = \frac{1}{\rho}\nabla \cdot \sigma \quad (1)$$

$$\nabla \cdot u = 0 \quad (2)$$

where u and σ respectively represent the fluid velocity vector and stress tensor, and ρ is the density. σ is defined by

$$\sigma = 2\eta\left(\dot{\gamma}\right)D + -pI \quad (3)$$

where η and denote the viscosity of blood and shear rate, respectively. p is the pressure. D is the rate of deformation tensor which is defined by

$$D = \mu\left[\nabla u + (\nabla u)^T\right] \quad (4)$$

where μ is the blood viscosity.

The vessel wall is assumed to be an isotropic, non-linear elastic material with no infiltration. The equation governing the solid domain:

$$\nabla \cdot \sigma_s = \rho_s \cdot \alpha_s \quad (5)$$

where σ_S is the stress tensor, ρ_S is the density, and a_S is the acceleration.

Mesh generation

Meshes were generated using ICEM software (ANSYS, Inc., Canonsburg, PA, USA). The geometric models were meshed using unstructured tetrahedral volume meshes. The minimum and maximum sizes of the mesh were 0.06 mm and 1 mm, respectively, for the fluid part of the model. Five layers of fine mesh with a height ratio of 1.2 were used. The size of the mesh was 0.1 mm for the solid part of the model.

Boundary conditions

In this study, the inlet flow velocity is set as a constant, which is a simple way to compare the different effects of normal right coronary arteries and abnormal right coronary arteries on haemodynamics. The maximum exit velocity of the left ventricle was set as the entry boundary condition for the numerical simulation, as denoted by the red dot in Fig. 2 [44].

Finally, the boundary conditions are set as follows:

(1) On the entry of the aorta, the tangential velocity is set to 1 m/s, and the normal velocity is set to 0 m/s.

V_t=1 m/s;

V_n=0 m/s.

where the subscripts t and n are angential and normalt directions, respectively.

(2) On the exits of the aorta, the normal and tangential outlet pressure is 0 Pa.

p_n=p_t=0 Pa;

The wall of blood domain is assumed to has no slip, v_n=v_t=0 m/s. Fluid-solid coupling follows the most basic conservation principle, so the conservation of fluid and solid stress, displacement and flow should

be met at the fluid-solid coupling interface.

$$\sigma_s \cdot n_s = \sigma_f \cdot n_f \quad (7)$$

$$d_s = d_f \quad (8)$$

where d is the displacement vectors, σ is the stress tensors, n is the boundary normal, and the subscripts f and s represent fluids and solids, respectively.

Numerical simulation

In the paper, a one-way fluid-solid coupling simulation was executed with ANSYS workbench. The finite volume method (FVM) mixed with the finite element method (FEM) is used to solve the governing equations. The structural analysis of vessel wall was solved with ANSYS Mechanical, and a CFD software based on the finite element method, ANSYS CFX (ANSYS CFX 19.0, Canonsburg, USA), was used for the fluid analysis of blood. The semi-implicit method for pressure linked equations consistent (SIMPLEC) algorithm was used to couple the outflow velocity term, and all equations were solved by the separation solution method. The convergence criterion was set to 1×10^{-4}.

According to the Reynolds number, for Re<2300, the flow of blood is set to laminar. Re is defined by:

$$Re = \frac{\rho v d}{\mu} \quad (1)$$

where v and ρ are the velocity and density of the fluid, respectively. d is the characteristic length, and μ is the viscosity of the fluid.

Statistical analysis

To eliminate the differences in patient specificity, multiple cases were analysed by statistical analysis. Statistical analysis was performed using GraphPad Prism (GraphPad Software 8.0, CA, USA). Correlation analysis was used to evaluate the relationship between area and flow rate, pressure and WSS. The difference in cross-sectional area of the inlet, volumetric flow, pressure and WSS between the two groups was studied by t-tests of two independent samples. The number in pressure and WSS was collected by means of the five-point sampling method. If correlation coefficient r was close to +1, 0 and -1, the results were positive correlation, negative correlation and no correlation, respectively. A correlation less than 0.5 was described as weak, whereas a correlation more than 0.8 was described as strong. The significance level was set at P<0.05.

Declarations

Ethics approval and consent to participate

Not applicable.

Abbreviations

LCA: the left coronary artery; RCA: the right coronary artery; AAOCA: Anomalous origin of the coronary artery ; AORL: anomalous origin of the right coronary artery from the left esinus; SCD: sudden cardiac death; IVUS: intravascular ultrasonography; CFD: computational fluid dynamics; CT: computed tomography; BMI: Body Mass Index; FVM: finite volume method; FEM: finite element method; SIMPLEC: semi-implicit method for pressure linked equations consistent; AAO: ascending aorta.

Acknowledgements

The authors would like to thank Academic promotion programme of Shandong First Medical University No. 2019QL009 for fnancial support, and Jianfeng Qiu was supported by the Taishan Scholars Program of Shandong Province, No. TS201712065.

Authors' contributions

SD, CC collected the experimental data. MC, XX, JQ, SQ and HZ reviewed literatures and discussed the method for this study. MC performed the experiments and drafted the manuscript. HZ, XX, JQ and SQ reviewed and edited the writing. All authors fnalized the manuscript for submission. All authors read and approved the fnal manuscript.

Funding

This work was supported in part by Academic promotion programme of Shandong First Medical University No. 2019QL009 and Jianfeng Qiu was supported by the Taishan Scholars Program of Shandong Province, No. TS201712065.

Availability of data and materials

The datasets used and/or analysed during the current study are available from the corresponding author on reasonable request.

Consent for publication

Not applicable.

Conflicting Interest

The authors declare that they have no conflict of interest.

References

1. Yuan S-M. Anomalous origin of coronary artery: taxonomy and clinical implication. Revista Brasileira de Cirurgia Cardiovascular. 2014;29:622-9.

2. Fathala A, Hassan W. Coronary artery anomalies: A diagnostic challenge. Journal of the Saudi Heart Association. 2011;23:37-9.
3. Ropers D, Moshage W, Daniel WG, Gottwik M, Achenbach S. Visualization of coronary artery anomalies and their anatomic course by contrast-enhanced electron beam tomography and three-dimensional reconstruction. The American Journal of Cardiology. 2001;87:193-7.
4. Scanlon PJ, Faxon DP, Audet A-M, Carabello B, Dehmer GJ, al e. ACC/AHA guidelines for coronary angiography. A report of the American College of Cardiology/American Heart Association Task Force on practice guidelines (Committee on Coronary Angiography) Developed in collaboration with the Society for Cardiac Angiography and Interventions. Games of the hangman. 1999;99:2345-57.
5. A P, JE J, F S, J L, AN M. Coronary cta assessment of coronary anomalies. Journal of Cardiovascular Computed Tomography. 2012;6:48-59.
6. Brothers JA. Introduction to anomalous aortic origin of a coronary artery. Congenital heart disease. 2017;12:600-2.
7. K X, Ç H. Anomalous Origin of Coronary Arteries. 2018.
8. Kragel AH, Roberts WC. Anomalous origin of either the right or left main coronary artery from the aorta with subsequent coursing between aorta and pulmonary trunk: Analysis of 32 necropsy cases. American Journal of Cardiology. 1988;62:771-7.
9. Fiorilli R, Menichelli M, De FF, Parma A, Violini R. Anomalous origin of the right coronary artery from the left sinus of Valsalva: case report and literature review. Giornale Italiano Di Cardiologia. 2007;8:123.
10. Jo Y, Uranaka Y, Iwaki H, Matsumoto J, Koura T, Negishi K. Sudden cardiac arrest: associated with anomalous origin of the right coronary artery from the left main coronary artery. Texas Heart Institute Journal. 2011;38:539-43.
11. G F, ER B, G T. Anomalous Coronary Artery Origin and Sudden Cardiac Death: Clinical and Pathological Insights From a National Pathology Registry. JACC Clinical electrophysiology. 2019.
12. MD C, CM DC, HA M. Sudden Death as a Complication of Anomalous Left Coronary Origin From the Anterior Sinus of Valsalva: A Not-So-Minor Congenital Anomaly. Circulation Cardiovascular Imaging. 1974;50:780-7.
13. K H, Y H, N M. Anomalous origin of the right coronary artery evaluated with multidetector computed tomography and its clinical relevance. J Cardiol. 2016;68:196-201.
14. Cubero A, Crespo A, Hamzeh G, Cortes A, Rivas D, Aramendi JI. Anomalous Origin of Right Coronary Artery From Left Coronary Sinus—13 Cases Treated With the Reimplantation Technique. World Journal for Pediatric & Congenital Heart Surgery. 2017;8:315-20.
15. Taylor AJ, Byers JP, Cheitlin MD, Virmani R. Anomalous right or left coronary artery from the contralateral coronary sinus: “High-risk” abnormalities in the initial coronary artery course and heterogeneous clinical outcomes. American Heart Journal. 1997;133:428-35.
16. Yamanaka O, Hobbs RE. Coronary artery anomalies in 126,595 patients undergoing coronary arteriography. Cathet Cardiovasc Diagn. 1990;21:28-40.

17. Angelini P, Vidovich MI, Lawless CE, Elayda MA, Lopez JA, Wolf D, et al. Preventing SuddenCardiac Death in Athletes In Search of Evidence-Based, Cost-Effective Screening. Tex Heart Inst. 2013;40:148-55.
18. Angelini P, Urrea JM, Forstall P, Ramirez JM, Uribe C, Hernandez E. Anomalous Right Coronary Artery from the Left Sinus of Valsalva: Pathophysiological Mechanisms Studied by Intravascular Ultrasound, Clinical Presentations and Response to Stent Angioplasty. Journal of the American College of Cardiology. 2013;61:E1804.
19. Ripley DP, Saha A, Teis A, Uddin A, Bijsterveld P, Kidambi A, et al. The distribution and prognosis of anomalous coronary arteries identified by cardiovascular magnetic resonance: 15 year experience from two tertiary centres. J Cardiovasc Magn Reson. 2014;16:34-42.
20. Driesen BW, Warmerdam EG, Sieswerda GJT. Anomalous coronary artery originating from the opposite sinus of Valsalva (ACAOS), fractional flow reserve- and intravascular ultrasound-guided management in adult patients. Catheterization and Cardiovascular Interventions. 2018.
21. Taylor CA, Figueroa CA. Patient-specific modeling of cardiovascular mechanics. Annual review of biomedical engineering. 2009;11:109-34.
22. Sun Z, Xu L. Computational fluid dynamics in coronary artery disease. Computerized Medical Imaging and Graphics. 2014;38:651-63.
23. Morris PD, Narracott A, Tengg-Kobligk Hv, Soto DAS, Hsiao S, Lungu A. Computational fluid dynamics modelling in cardiovascular medicine. Heart. 2016;102:18-28.
24. Tian X, Sun A, Liu X, Pu F, Deng X. Influence of catheter insertion on the hemodynamic environment in coronary arteries. Medical Engineering & Physics. 2016.
25. Liu X, Peng C, Xia Y, Gao Z, Xu P, Wang X, et al. Hemodynamics analysis of the serial stenotic coronary arteries. Biomed Eng Online. 2017;16:127.
26. Zhou Y, Tong J, Li X, Li X, Wang G. Numerical simulation of haemodynamics and low-density lipoprotein transport in the rabbit aorta and their correlation with atherosclerotic plaque thickness. Journal of the Royal Society Interface. 2019;14:20170140.
27. Chaichana T, Sun Z, Jewkes J. Computation of hemodynamics in the left coronary artery with variable angulations. Journal of biomechanics. 2011;44:1869-78.
28. Wu J, Liu G, Huang W, Ghista DN, Wong KKL. Transient blood flow in elastic coronary arteries with varying degrees of stenosis and dilatations: CFD modelling and parametric study. Computer Methods in Biomechanics & Biomedical Engineering. 2015;18:1835-45.
29. Cho SH, Joo HC, Yoo KJ, Youn YN. Anomalous Origin of Right Coronary Artery from Left Coronary Sinus: Surgical Management and Clinical Result. Thorac Cardiovasc Surg. 2014;63.
30. Poynter JA, Williams WG, McIntyre S, Brothers JA, Jacobs ML, Congenital Heart Surgeons Society AWG. Anomalous aortic origin of a coronary artery: a report from the Congenital Heart Surgeons Society Registry. World J Pediatr Congenit Heart Surg. 2014;5:22-30.
31. Izgi C, Feray H, Erdem G, Kaya Z. Anomalous origin and interarterial course of right coronary artery associated with angina and proven ischemia. The International journal of angiology : official

publication of the International College of Angiology, Inc. 2014;23:271-4.
32. Y H, K K, K K, N I, N N. Anomalous origin of the right coronary artery from the left coronary sinus with an intramural course: comparison between sudden-death and non-sudden-death cases. Cardiovascular Pathology. 2014;24:154-9.
33. Lameijer H, Ter Maaten JM, Steggerda RC. Additive value of dobutamine stress echocardiography in patients with an anomalous origin of a coronary artery. Netherlands heart journal : monthly journal of the Netherlands Society of Cardiology and the Netherlands Heart Foundation. 2015;23:139-40.
34. Crossman DC. The pathophysiology of myocardial ischaemia. Heart. 2004;90:576-80.
35. Kamangar S, Badruddin IA, Ameer Ahamad N, Soudagar MEM, Govindaraju K, Nik-Ghazali N, et al. Patient specific 3-d modeling of blood flow in a multi-stenosed left coronary artery. Bio-Medical Materials and Engineering. 2017;28:257-66.
36. Ferri FF. FERRI'S CLINICAL ADVISOR 2016. 1920.
37. Wilson J, Harrison T, Isselbacher K, Gwowdon J, Fink J, Isselbacher K. Harrison's Principles of Internal Medicine. Practitioner. 2001;204:831-7.
38. Zhang JM, Zhong L, Su B, Wan M, Yap JS, Tham JP, et al. Perspective on CFD studies of coronary artery disease lesions and hemodynamics: a review. International journal for numerical methods in biomedical engineering. 2014;30:659-80.
39. Gijsen F, van der Giessen A, van der Steen A, Wentzel J. Shear stress and advanced atherosclerosis in human coronary arteries. Journal of biomechanics. 2013;46:240-7.
40. Zhang B, Gu J, Qian M, Niu L, Ghista D. Study of correlation between wall shear stress and elasticity in atherosclerotic carotid arteries. Biomed Eng Online. 2018;17:5.
41. Sadeghi MR, Shirani E, Tafazzoli-Shadpour M, Samaee M. The effects of stenosis severity on the hemodynamic parameters-assessment of the correlation between stress phase angle and wall shear stress. Journal of biomechanics. 2011;44:2614-26.
42. Zhao SZ, Xu XY, Hughes AD, Thom SA, Stanton AV, Ariff B, et al. Blood flow and vessel mechanics in a physiologically realistic model of a human carotid arterial bifurcation. 2000;33:975-84.
43. Saeed B, Mahmood N. A numerical study on hemodynamics in the left coronary bifurcation with normal and hypertension conditions. Biomechanics & Modeling in Mechanobiology. 2018;17:1785-96.
44. Bongert M, Geller M, Pennekamp W. Transient simulation of the blood flow in the thoracic aorta based on MRI-data by fluid-structure-interaction. 4th European Conference of the International 2009.

Table

Table 1 Scan settings

Parameter	Value
Rotation speed	280 ms/r
Collimator	2×128×0.6 mm
Slice thickness	0.75 mm
Slice increment	0.50 mm
In plane resolution	512×512

Figures

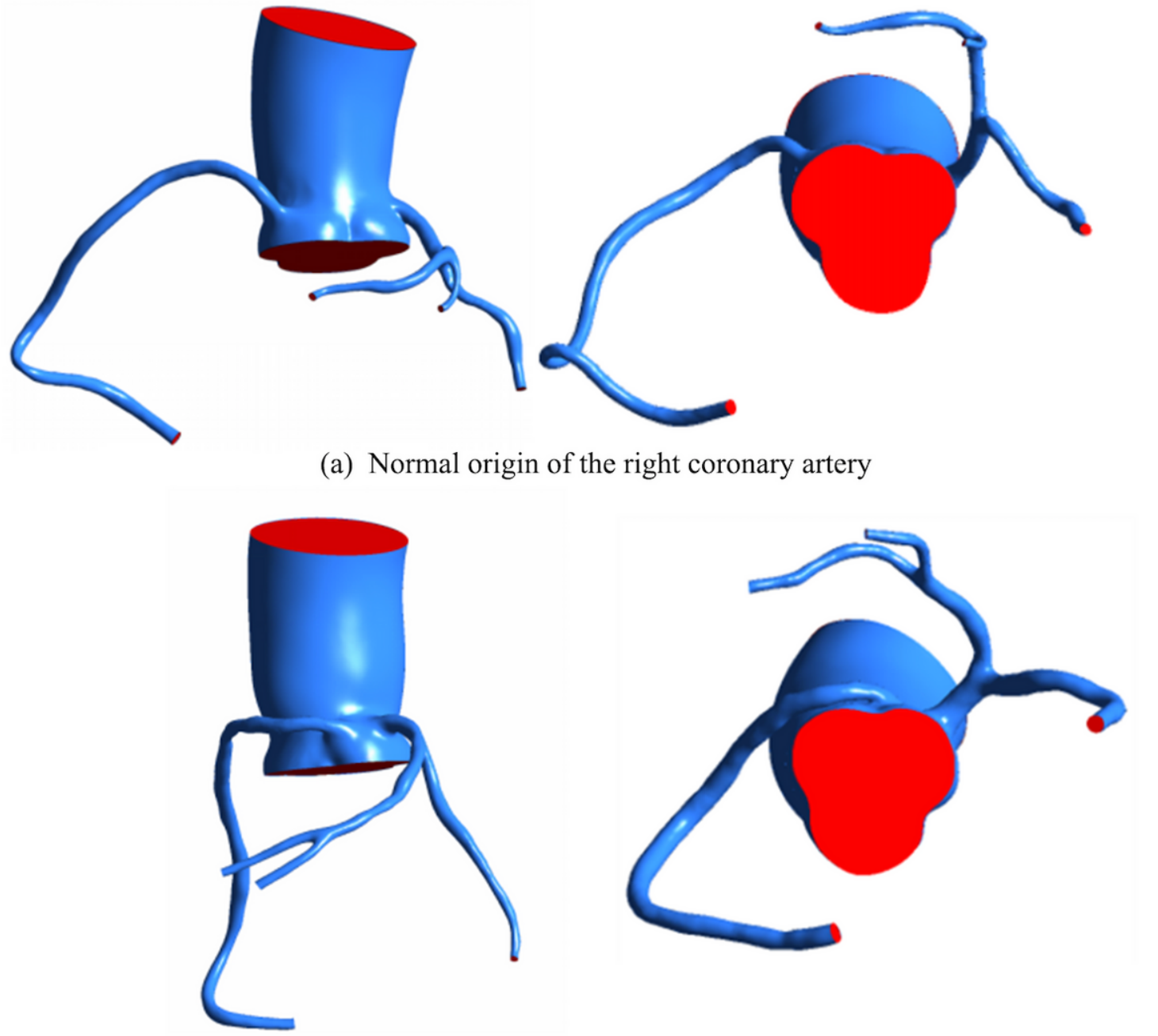

Figure 1

Two examples of coronary artery models are shown in the front view and the upward view.

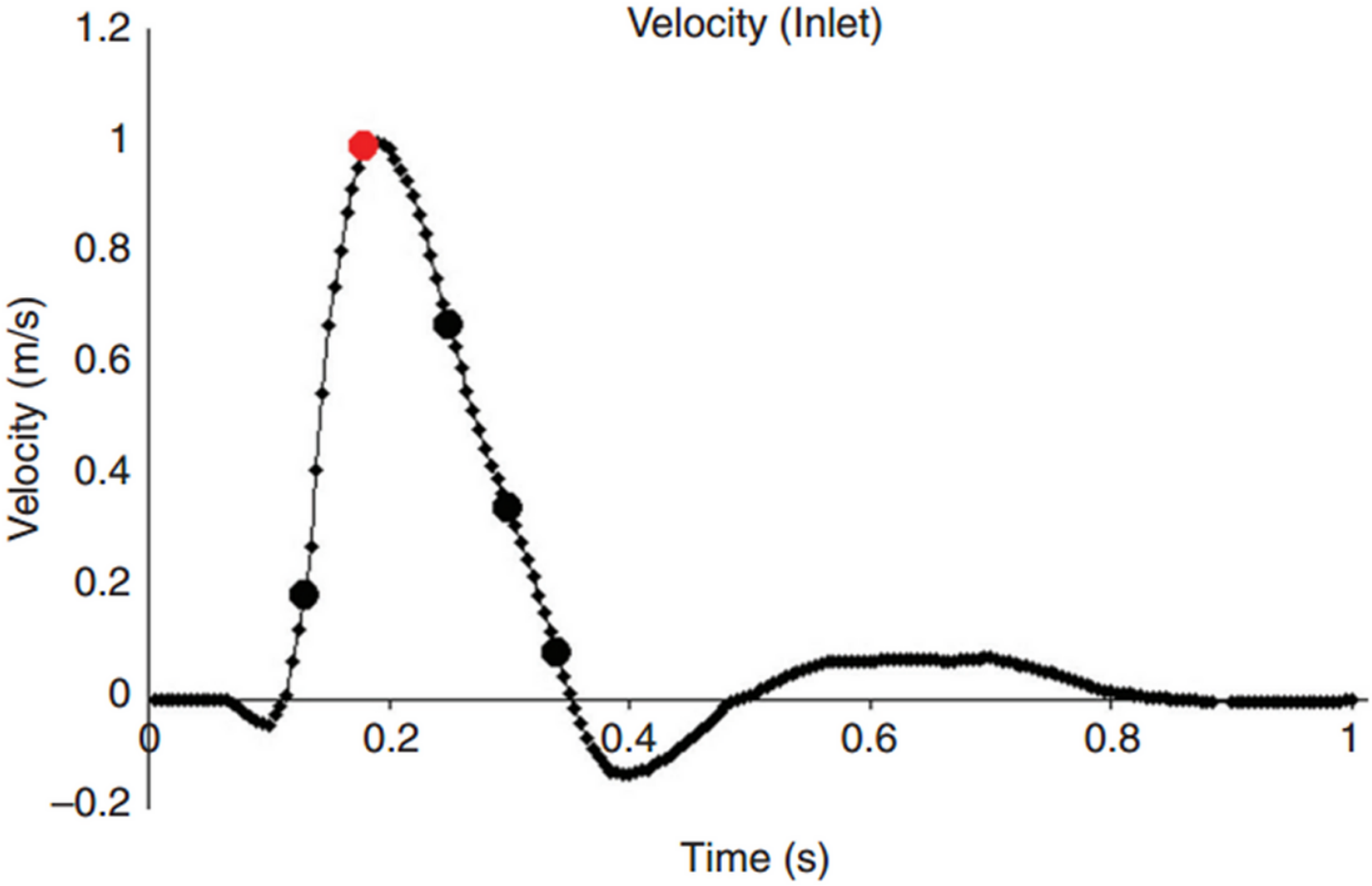

Figure 2

The exit velocity of the left ventricle is measured during a complete heart cycle. For stationary simulation, the entry boundary condition chosen the maximum velocity. The velocity is 1.0 m/s.

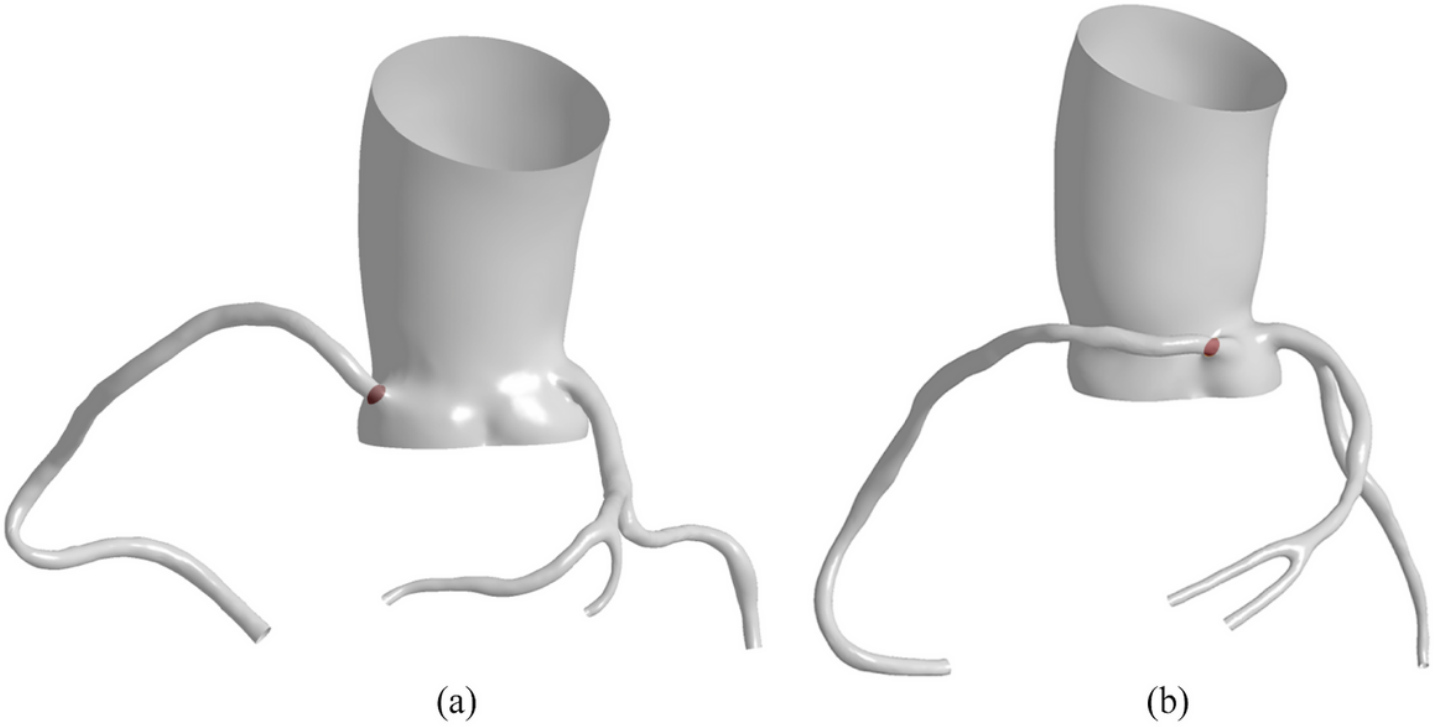

Figure 3

The position of the right coronary artery inlet velocity. (a) Normal origin of the right coronary artery, (b) Anomalous origin of the right coronary artery from the left coronary sinus of Valsalva. Two examples are used to indicate the location of the entrance.

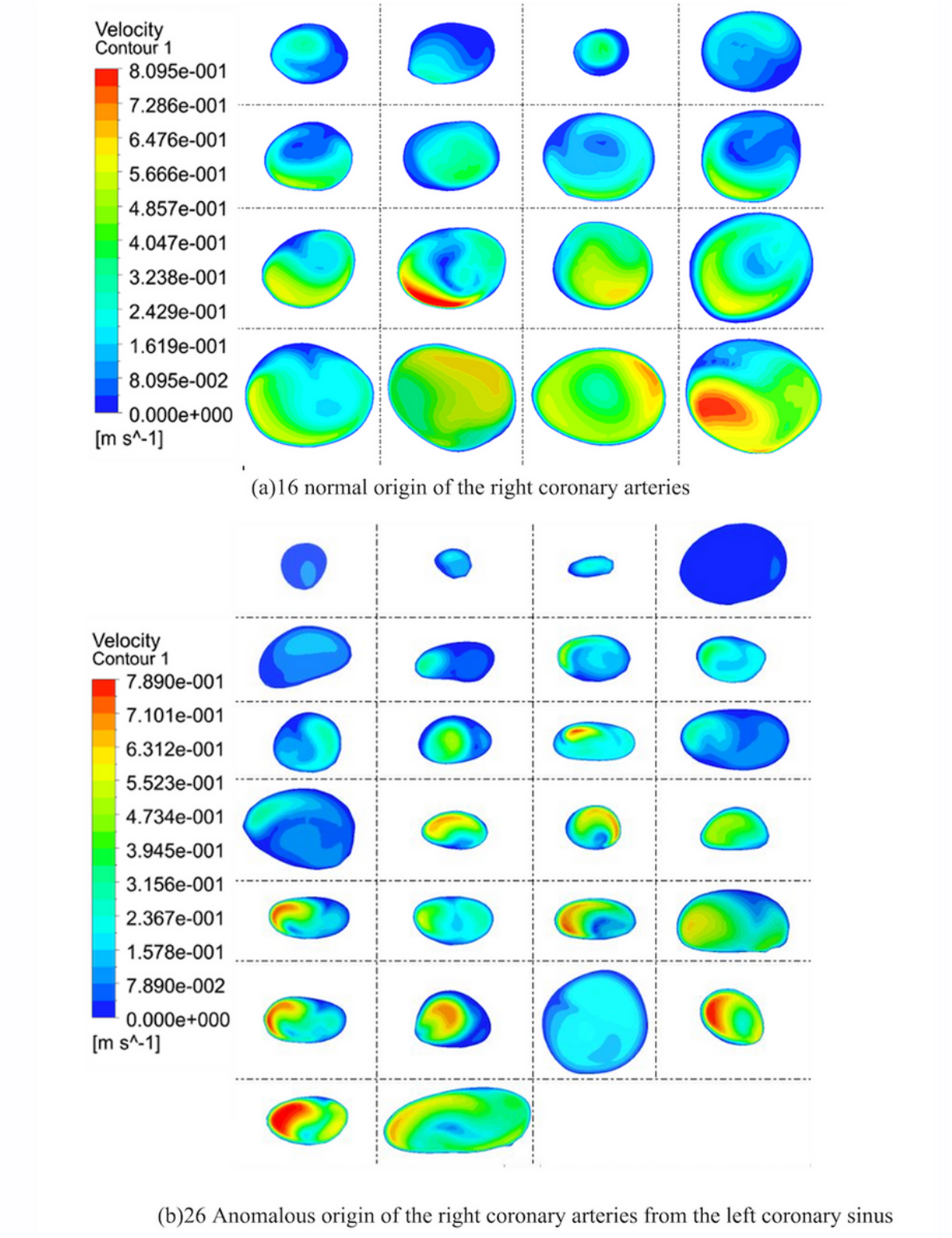

Figure 4

Flow rate of the entrance section of the right coronary artery. Due to individual differences, the area and shape of the entrance section of each model are different. The flow of the inlet section of each of the normal and anomalous group could be read separately by two contours.

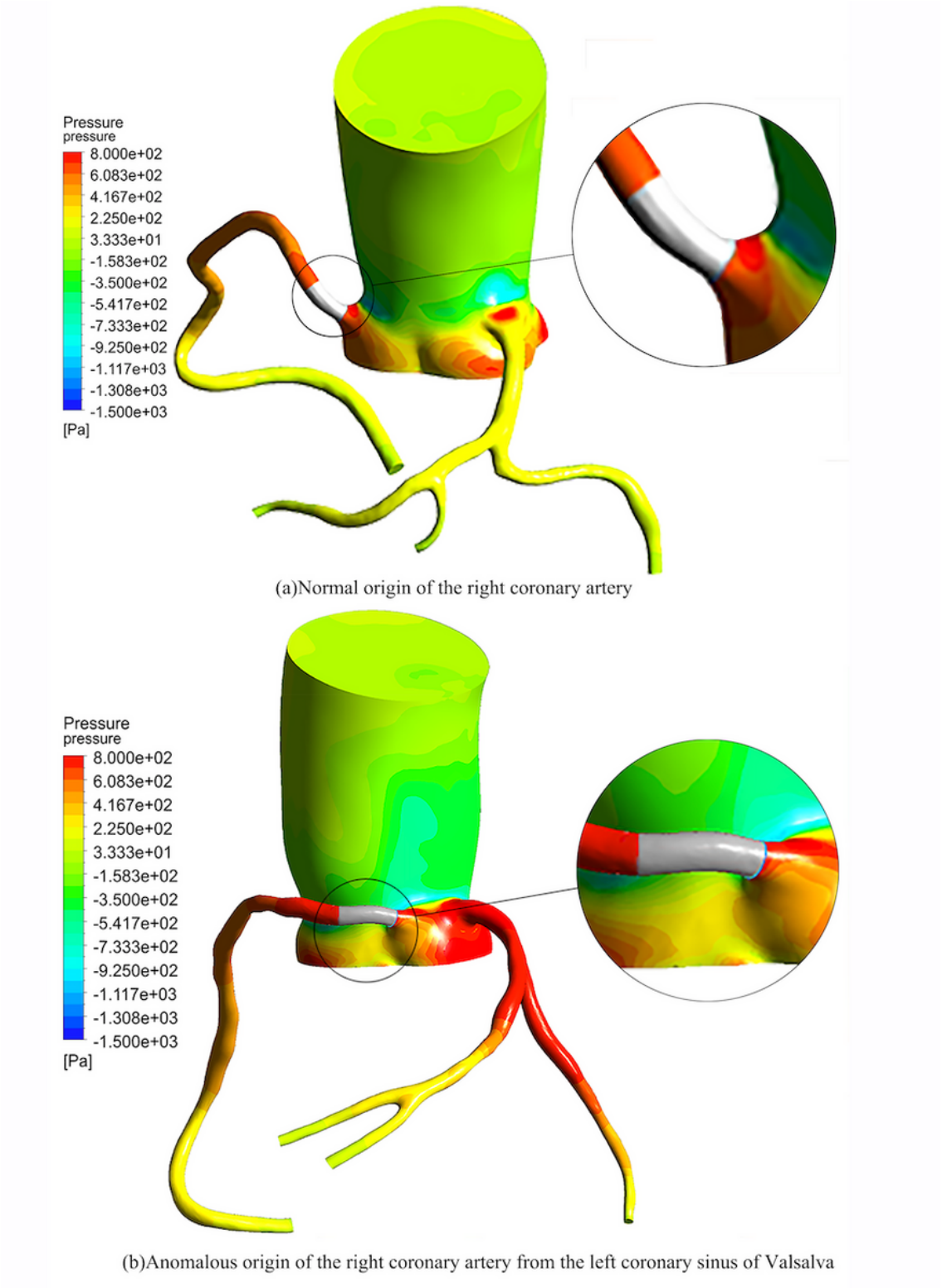

Figure 5

The location selected by the five-point sampling method. The gray area is the value area of the model, and the value area is enlarged 4 times to show the details.

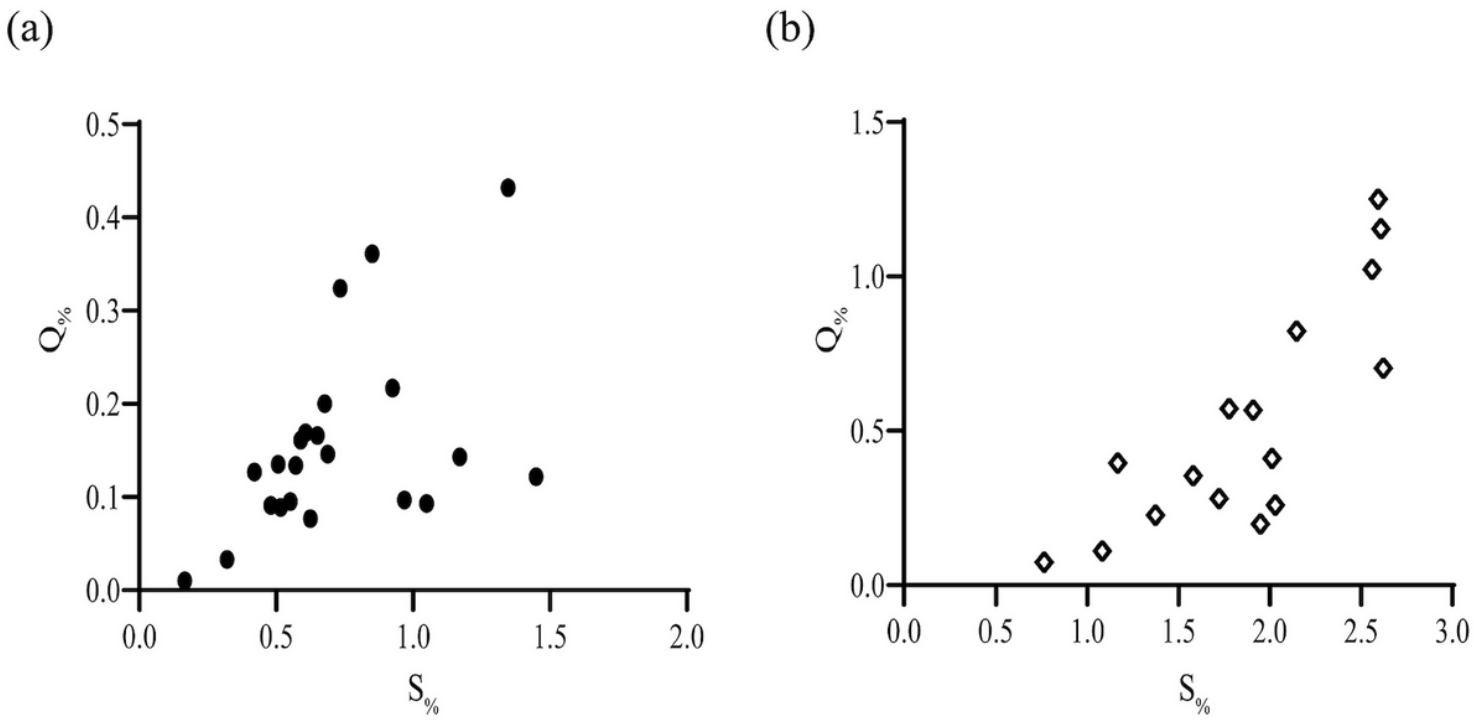

Figure 6

(a) Normal origin of the right coronary artery, (b) Anomalous right coronary artery from the left coronary artery sinus. S% is the ratio of the cross-sectional area of the right coronary artery to the inlet area of the ascending aorta. Q% is the ratio of the inlet volumetric flow of the right coronary artery to the volumetric flow of the ascending aorta.

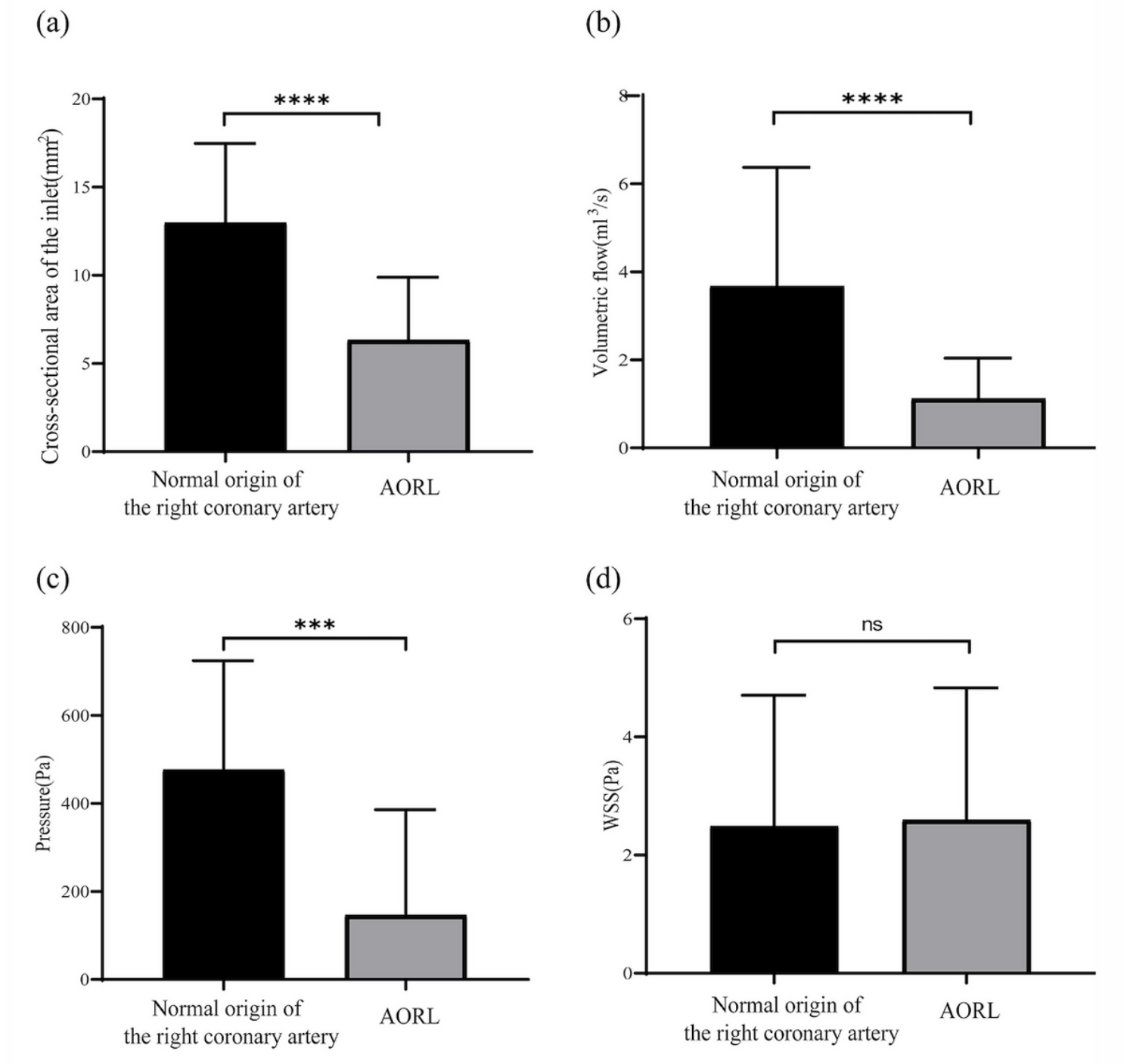

Figure 7

The figure shows the comparison of inlet cross section area, volume flow, pressure and WSS between the abnormal group and the normal group. ****P<0.0001,***P=0.0001, ns P>005.